Journal of
Manufacturing and Materials Processing

MDPI

Article

Development of Polymer Hydrophobic Surfaces Through Combined Laser Ablation and Hot Embossing Processes

Esmaeil Ghadiri Zahrani [1,2], Amirmohmmad Fakharzadeh Jahromi [1] and Bahman Azarhoushang [1,*]

[1] Institute for Advanced Manufacturing (KSF), Furtwangen University, 78532 Tuttlingen, Germany; esmaeil.ghadiri.zahrani@hs-furtwangen.de (E.G.Z.); amirmohammad.fakharzadehjahromi@hs-furtwangen.de (A.F.J.)
[2] Department of Microsystems Engineering (IMTEK), University of Freiburg, 79110 Freiburg, Germany
* Correspondence: aza@hs-furtwangen.de

Abstract: The development of hydrophobicity on polymer surfaces in mass production is one of the most critical challenges in the plastic industry. This paper deals with a novel combined hot embossing process in which femtosecond laser ablation is utilized to texture the embossing stamps. By controlling the process temperature and axial forces, the laser textures were transferred to polymer surfaces, successfully resulting in hydrophobicity. Four different polymers, including ABS, PP, PA, and PC, along with two different laser textures, namely ball and pyramid, were tested. The laser and hot embossing parameters under which the textures were transferred to the polymers are introduced. The critical micro- and nano-features of the transferred textures that resulted in high hydrophobic contact angles are also discussed. The results indicate that PP and ABS have higher contact angles, respectively, while under the given parameters, PA and PC did not exhibit hydrophobic surfaces.

Keywords: polymer; hydrophobicity; femtosecond laser ablation; hot-embossing; micro- and nano-features

Citation: Ghadiri Zahrani, E.; Fakharzadeh Jahromi, A.; Azarhoushang, B. Development of Polymer Hydrophobic Surfaces Through Combined Laser Ablation and Hot Embossing Processes. *J. Manuf. Mater. Process.* **2024**, *8*, 262. https://doi.org/10.3390/jmmp8060262

Academic Editor: Shuo Yin

Received: 24 October 2024
Revised: 11 November 2024
Accepted: 19 November 2024
Published: 20 November 2024

1. Introduction

Hydrophobicity, the property of repelling water, plays a crucial role in various applications. Surfaces with high hydrophobicity exhibit low water adhesion and are often characterized by water droplets forming spherical shapes or sliding off effortlessly with high values of contact angles [1].

Surface energy and roughness are the major contributing factors that determine whether a surface is wetting or non-wetting [2]. The exploration of wettability holds promise in designing self-cleaning surfaces [3] and surfaces with enhanced adhesive resistance [4]. Various techniques, such as photolithography [5], laser interference lithography [6], chemical etching [7], and layer-by-layer assembly [8], can be employed to create hydrophobic surfaces. However, these methods come with drawbacks, including multiple steps, the use of additional materials, and time-consuming processes, all contributing to increased costs.

To overcome these challenges, laser processing technology proves to be an effective technique for producing surfaces with nano- and micro-structures [9,10]. During the laser ablation process, the target material absorbs laser energy, melts, and evaporates, which causes morphological changes inside and around the ablation area [11]. Through the laser ablation process, different structures can result in hydrophobicity [12]. In one study, hydrophobicity on AISI 430 stainless steel was achieved in three laser patterns: octagonal donut patterns, ellipses at 90° angles, and a dimple array. The structure of ellipses at 90° angles showed a contact angle of 98° [13]. Both the structure type and the laser parameters are extremely important in producing hydrophobicity. The surface transitioned from hydrophilic to hydrophobic and eventually became superhydrophobic when laser processing was conducted at the highest repetition rate [14]. The stability of hydrophobicity on laser-textured surfaces is another criterion that is influenced by the laser fluence. It

is shown that structured surfaces achieve stable hydrophobic conditions when the peak fluence exceeded a threshold, resulting in final contact angles above 140°. Conversely, when the fluence was below this threshold, the surface initially became hydrophobic, reaching a maximum contact angle, but its hydrophobicity diminished over time [15]. Although direct laser processing is a promising technique compared to other methods to produce hydrophobicity, the process represents some surface damages and it is still not an economical method for some industrial application. In the direct ablation process of polymers, a significant amount of energy is absorbed by the material, leading to heating, boiling, vaporization, and the formation of pores. These pores observed that the following laser ablation can be attributed to the rapid cooling of the superheated melt after intense boiling [16]. The presence of pores can negatively impact the performance of a final part, particularly if it is intended for use in harsh and abrasive environments. Therefore, the selection of laser parameters significantly influences the final performance. For instance, in terms of hydrophobicity, polymers exhibit different responses to various laser parameters. For example, PEEK displays varying contact angles depending on the laser wavelength: untreated PEEK has a contact angle of 92.4°, and laser treatment yield angles of 59.5° at 1064 nm, 131.0° at 532 nm, and 52.5° at 355 nm [17]. Therefore, a much more robust process is desirable. Combining laser processing with other methods, for example, hot embossing could be an alternative for producing hydrophobicity. Hot embossing is an intriguing process due to its ability to replicate fine micro- and nano-scale details with high precision and cost-effectiveness compared to other microfabrication techniques. It accommodates a variety of thermoplastic materials and can be scaled from small to large production volumes, making it suitable for industrial manufacturing. The process enhances material properties, such as lubricity. Advances in hot embossing technology have reduced cycle times and improved efficiency, enabling faster quicker production and lower costs [18].

Y. Gong et al. [19] focused on creating a superhydrophobic surface using PTFE/graphite composites through a hot embossing process. The surface morphology was analyzed by measuring the structural parameters of the replicated protrusions. The study further investigated the effects of embossing temperature and time on the polymer filling mechanism. Due to graphite's excellent lubricity, nanoscale mold cavities were filled efficiently, reducing the embossing time and enhancing mass production viability. Lowering the embossing temperature mitigates the impact of submicron fibers on the mold service life. Optimal process conditions were recommended to achieve hydrophobicity.

J. Sun et al. [20] explored the use of stainless steel stamps to create polymeric superhydrophobic surfaces with biomimetic hierarchical roughness through isothermal hot embossing. The resulting surfaces featured micro-platforms and microfibers formed during molding. This resulted in a water contact angle of 154° and an oil contact angle of 97°, which increased to 140° after fluorosilane modification. Water droplets rolled off the surface at a tilt of approximately 1°, indicating a very low sliding angle.

J. J. Victor et al. [21] introduced a template-based method for the creation of superhydrophobic polymer surfaces. The process structured PE, PP, and PTFE samples, creating nano-scale roughness on micro-scale protrusions, significantly increasing the contact angles and reducing the tilt angles. The effects of temperature, droplet size, and surfactant concentration on the wetting properties were also examined. Despite slight decreases in contact angles with increased droplet size and temperature, the surfaces remained hydrophobic up to 90 °C. High surfactant concentrations reduced hydrophobicity, but the pressed PTFE remained hydrophobic.

H.J. Lee et al. [22] introduced a repetitive ultrasonic embossing technique to create composite micro-patterns using a simply patterned mold. The process utilized ultrasonic imprinting to locally soften the polymer surface. This method was also used to fabricate composite micro-patterns combining prism and pyramid shapes on a single-polymer film.

In almost all the methods mentioned above, the efficiency of hydrophobicity is partial and depends on many factors such as stamp geometry, material properties, parameter variation, fillers, and other variables, making the optimization of parameters a complex

problem. Therefore, it would be very useful to have a more tangible and applicable hot embossing method to avoid any uncertainty. In order to achieve this particular aim, in this study, a hybrid method of laser structuring and hot embossing is presented. Based on this explanation, as far as the authors know, there has been no prior publication on a hybrid process at an industrial level similar to our work. In this study, laser processing is employed to structure the stamp used in the embossing process. Various patterns were meticulously applied to the stamp to transfer texturing, which is explained in the next sections.

2. Experimental Set-Up

Figure 1 illustrates the sequential steps involved in the process of generating hydrophobic surfaces and assessing the hydrophobic properties of a polymer using a textured stamp. The process begins with the preparation stage, where a stamp without structure is prepared, and its surface roughness is measured to ensure the specific roughness quality. This is followed by the laser processing stage, which involves setting up the ultra-short-pulse laser machine, selecting appropriate laser parameters, and choosing a laser pattern to create the desired texture on the stamp. Once the laser processing is complete, the next stage is analyzing the texture of the stamp to determine its geometrical characteristics. Afterwards, the hot embossing process transfers the texture from the stamp to the polymer by applying force and temperature for a specific holding time. The detailed evaluation follows the analysis of the transferred texture on the polymer and measuring the contact angle.

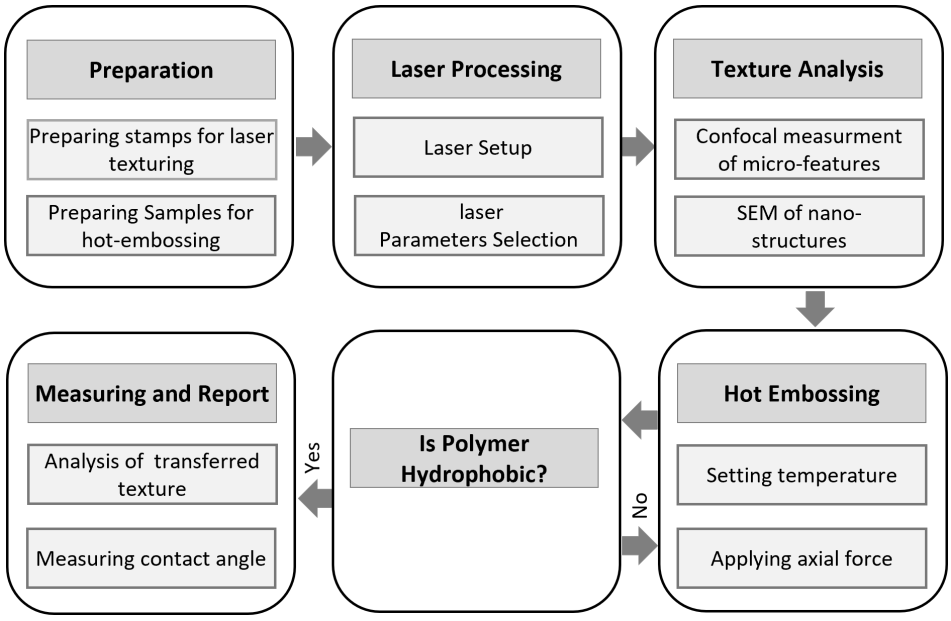

Figure 1. Overview of utilized steps for the combined processes of laser ablation and hot embossing.

The laser source employed was a solid-medium type known as Carbide-Model (CB3-40-0200-10-HB) from Light Conversion Company, Lithuania, with a wavelength of 1064 nm. The intensity profile of the laser beam was near-Gaussian ($M^2 < 1.2$), and the beam spot size ($2w_0$) was 22 µm. The laser system generates different infrared pulse widths, including tp = 750 fs, with a maximum average power output of 40 W. The laser source has been integrated into a 5-axis machine (+GF + LP400U), as shown in Figure 2a. The laser spot is positioned on the workpiece in nominal focus distance (F.D). The focus distance was kept in the nominal value of the F-theta lens equal to 100 mm. The used material is a disc (Ø28 × 12 mm) from stainless steel DIN1.4301 (Cr:17.5 to 19%, Ni: 8 to 10.5%, C < 0.07%_ Si < 1.0%_ Mn < 2.0%_ Pb < 0.045%_ S < 0.015%), which was machined before the laser machining. The initial surface roughness of the stamp and polymer workpieces was assessed using a tactile measurement instrument (Hommel-Etamic T 8000 by Jenoptik), with values of Ra = 1.38 µm (Rz = 7.79 µm) and Ra = 1.62 µm (Rz = 6.86 µm), respectively.

A confocal microscope (NanoFocus Mobile μsurf) was used to measure the geometrical micro-features of the laser textures.

Figure 2. (**a**) Five-axis laser machine; (**b**) Positioning of stamp; and (**c**) Dimensions of laser-textured stamp.

The laser parameters used in this study are given in Table 1. The experiments were conducted in ambient air, and all the experiments were conducted three times. Screening tests for the final parameters had already been completed successfully. These tests encompassed a thorough examination of each parameter to ensure low thermal damage and the generation of nanostructures on micro-patterns.

Table 1. Laser parameter.

Average Power (W)	**3.2**
Frequency (kHz)	600
Scanning speed (mm/s)	2000
Laser pulse width (fs)	750
Jump speed (mm/s)	3500
Number of repetitions	80
Hatch distance (μm)	20

Laser experimentation was conducted with two surface texture patterns, as represented in Figure 3. These patterns were used for laser texturing due to their symmetrical properties. All these patterns create air pockets that can repel water, making the surface less prone to wetting. Figure 2c shows a laser-structured stamp in which two rectangles with dimensions of 18 × 8 mm were lasered. These dimensions ensure a sufficient sliding path for hydrophobicity tests.

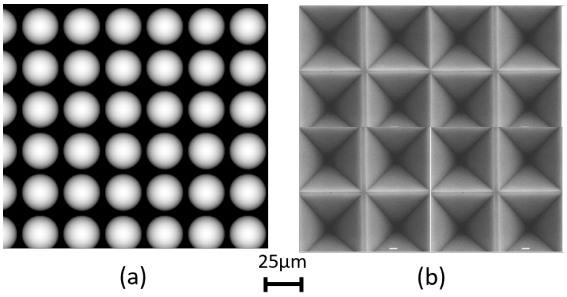

Figure 3. Patterns used for laser texturing: (**a**) Ball and (**b**) Pyramid.

Four types of polymers of ABS (acrylonitrile butadiene styrene), PP H (polypropylene), PC (polycarbonate), and PA (polyamide), were used as workpieces with dimensions of Ø28 × 10 mm. Table 2 summarizes the properties of the used polymers. The polymer workpieces were positioned between the laser-textured stamp and the holder ring, as illustrated in Figure 4.

Table 2. Polymers types and specification [23].

Polymer Type	ABS	PP	PC	PA
Glass transition temperature (°C)	85/104	−18	150	47–70
Melting point temperature (°C)	up to 230	165	260	220
Hardness (N/mm²)	74	120	120	80

Figure 4. Hot embossing set-up.

In the hot-embossing setup (Figure 4), the stamp is positioned inside a holding ring which is connected to a load cell for measuring the axial force applied on the stamp by a load screw. A heating element was also inserted in the holding ring to provide the required temperature for the stamp. The temperature was also controlled via a regulator to ensure that the working temperature does not exceed the defined threshold. The temperature range was selected below the melting point of the polymer (Table 2). A holding time of 60 s was applied for all the workpieces during the hot embossing process. To determine the range of the hot-embossing parameters, some screening tests were conducted, and based on the initial results, the parameters in Table 3 were adopted. To measure the contact angle on the polymer workpieces, an optical analysis system (DataPhysics—OCA 200) with distilled

water was utilized. The water volume used to measure the contact angle was between 7 and 8 µL.

Table 3. Hot-embossing parameter.

Parameter	Laser Textures & Polymers							
	Ball				Pyramid			
	ABS	PP	PC	PA	ABS	PP	PC	PA
Stamping temperature (°C)	120	160	120	190	120	160	120	190
Axial load (kg)	300	600	600	600	300	600	600	600
Holding time (s)	60	60	60	60	60	60	60	60

3. Results

Figure 5a shows the confocal images of the laser textures on the stamps as well as the micro-geometries that are transferred to the polymer surfaces. Comparing these images indicates that, for both ABS and PP, the micro-features are transferred almost one by one, while for PC and PA, the transformation is not complete. To compare and quantify these textures together, it is necessary to characterize the geometrical features of the structures. Figure 5b represents these features, and they are summarized in Table 4. The micro-features measured are height (A), landing length (B), width (C), peak-to-peak distance (D), and valley-to-valley distance (E). Overall, for the stamps, the pyramid texture exhibits the largest values in height, width, and valley-to-valley distance, while the ball texture tends to have lower measurements across the tip and peak-to-peak distance.

Table 4. Comparison between the micro-features of the laser-textured stamp and the hot-embossed polymer workpieces.

Micro-Feature	Laser Textures and Polymers									
	Ball					Pyramid				
	Stamp	ABS	PP	PC	PA	Stamp	ABS	PP	PC	PA
A (Height) [µm]	15.4	19	10	6.6	3	21.6	18.3	22.7	5.4	1.4
B (Landing length) [µm]	12	11	10.6	5.2	4.1	13.6	14.3	14.1	3.1	1.9
C (Width) [µm]	19	23.1	25.7	8.3	5	27	28.8	28.2	4.5	2.8
D (Peak to peak) [µm]	31.3	30.7	37.6	34.3	33.8	36	40.1	37.9	36.3	35.6
E (Valley to valley) [µm]	30.4	32.6	34.1	33.2	31.5	38.1	37.2	39.2	37.2	36.2

Based on the values in Table 4, all the micro-features of the stamp in the ball and pyramid textures were transferred for both ABS and PP polymers, while for PC and PA, these features were not transferred completely, despite a higher axial load and temperature being applied compared to ABS and PP. The differences in the transfer of micro-features in the hot embossing process could be attributed to several factors related to the thermal and rheological properties of these polymers. PC and PA have higher glass transition temperatures compared to ABS and PP, meaning that, at the applied temperature, these polymers might not soften enough to flow and conform to the micro-features of the stamp. Compared to ABS and PP, PC and PA generally have lower thermal conductivities; therefore, the temperature at the interface between the polymer workpiece and the stamp was not conducted uniformly. In addition, PC and PA have higher viscosities due to strong intermolecular forces and hydrogen bonding, respectively. ABS, as an amorphous polymer, does not have a crystalline structure that needs to be broken down [24]. This contributes to better flow characteristics at lower pressures.

By conducting hydrophobicity tests as shown in Figure 6, the contact angles for all the polymer surfaces as well as the stamp are summarized in Table 5. For the ABS material, the contact angle significantly increased from 43.9° without texture to 105.4° with the ball texture and slightly decreased to 94.0° with the pyramid texture. Similarly, for the PP material, the contact angle increased from 80.95° without texture to 118.2° with the ball texture and then slightly decreased to 112.0° with the pyramid texture. These results indicate that the ball texture generally leads to the highest contact angles for both ABS and PP, suggesting a greater hydrophobic effect with this texture compared to the pyramid and untextured surfaces.

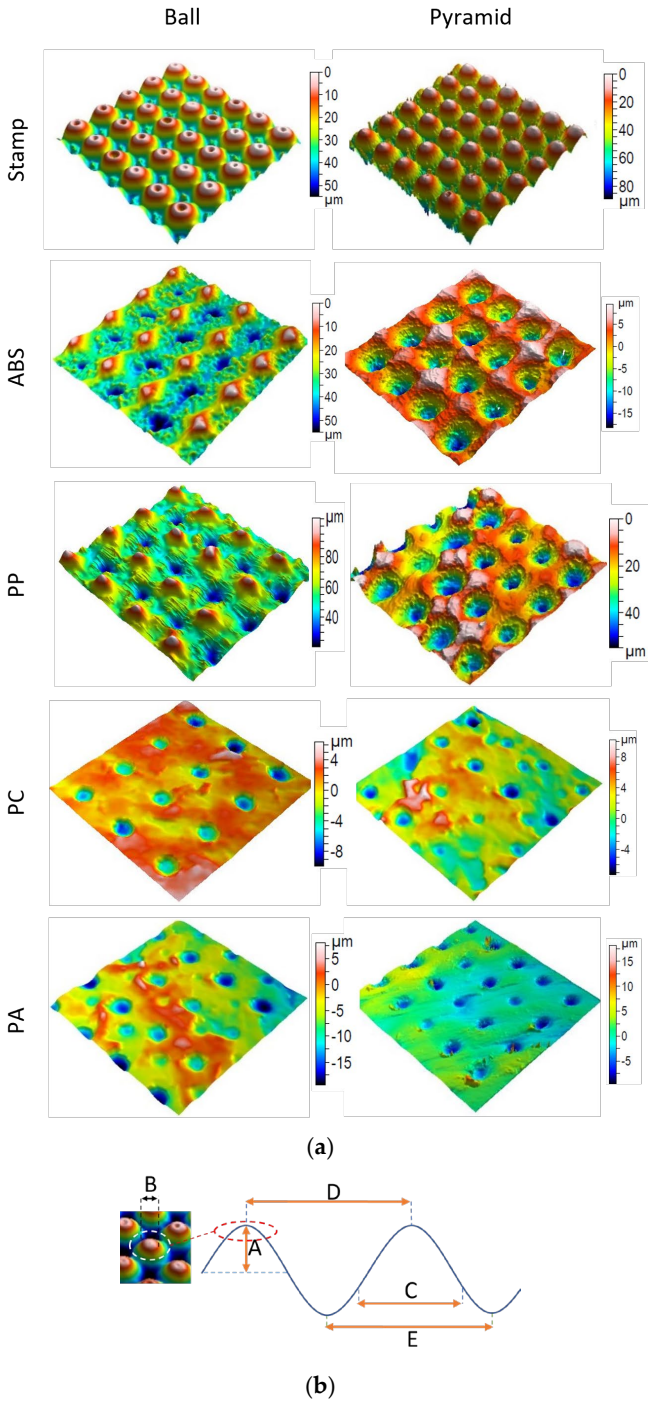

Figure 5. (**a**) Confocal images of the laser-textured stamps and (**b**) the 2D illustration of micro-features.

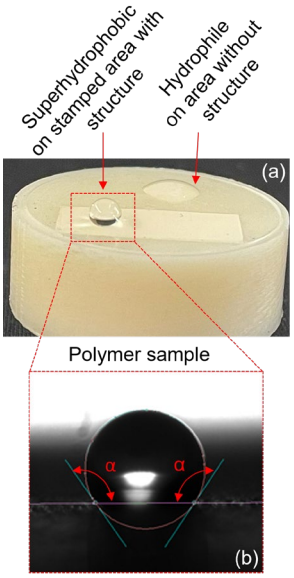

Figure 6. (**a**) Comparison between hydrophobic and hydrophile areas and (**b**) Measurement of contact angle.

Table 5. Contact angle measurements.

Texture	Material				
	Stamp	**ABS**	**PP**	**PC**	**PA**
Without texture	58°	43.9°	80.95°	68.2°	53.8°
Ball texture	90.8°	105.4°	118.2°	74.8°	65.5°
Pyramid texture	100.2°	94.0°	112.0°	85.7°	83.8°

Considering the contact angles (Table 5), the results in Table 4 indicate that achieving hydrophobicity requires surpassing a critical value for the geometrical micro-features, specifically for the height (A), landing length (B), and width (C). These geometrical features for both the laser textures of ball and pyramid can be defined as determining features. ABS with the pyramid texture achieves the highest height (22.7 µm), while PA with the ball texture shows the smallest height (1.4 µm). The pyramid texture on ABS yields the widest features (28.8 µm), while the PA with the ball results in the narrowest (2.8 µm). The pyramid consistently leads to larger distances compared to ball features, with slight material-dependent variation. Features for both textures tend to shrink (in terms of height, width, and spacing) as the material changes from ABS → PP → PC → PA. PA consistently has the smallest features across all measurements, indicating that it may be less receptive to deep or wide laser-textured features, while the ABS is more conducive to achieving pronounced textures. If the value of these features is met or exceeded after hot embossing, the surface becomes hydrophobic. If the geometrical features are smaller than the threshold values, the final transferred laser texture on the polymer surfaces does not result in hydrophobicity. The shape, depth, and spacing of the micro-features are crucial. For instance, deeper and narrower pockets can trap air more effectively, enhancing the stability of the Cassie–Baxter state, while shallow and wide pockets might not trap air as efficiently [25].

Increased roughness typically enhances hydrophobicity by trapping more air and reducing the contact area between the water and the solid surface. In fact, the morphology of the surface plays a significant role in this situation. To assess the effect of the surface morphology of the ablated area, a series of images was captured from the ablated texture using a scanning electron microscope (SEM-Zeiss, Crossbeam 550 L) (Figure 7). For both the ball and pyramid textures, the same nanostructures (Figure 7c,d) were observed. This is due to the fact that the same laser parameters were used for both structures; hence,

the conditions for melt formation were identical. Vertically aligned ridges, as shown in Figure 7d, can effectively trap air, maintaining high contact angles and reducing the contact area between the liquid and the solid surface. These structures have a high aspect ratio, such that the height of the melt particles formed after laser ablation is larger than their average diameter; however, extremely high aspect ratio structures might be mechanically fragile. After the hot embossing process, the status of the nanostructures was again investigated. The results indicate that, due to the applied load on the nanostructures during the hot embossing process, the nanostructures tended to be flattened, as shown in Figure 7e. Evaluating the nanostructures of the stamp surface is very important from the perspective of whether the nanostructures or the micro-features of the laser textures are more decisive in the hydrophobicity of the polymer surfaces. Since the nanostructures were flattened after the first hot embossing experiment, and the stamps were utilized several times for the hot embossing tests, and the surfaces of the polymers remained hydrophobic despite the fact that it indicates that the micro-features are more important than the nanostructures.

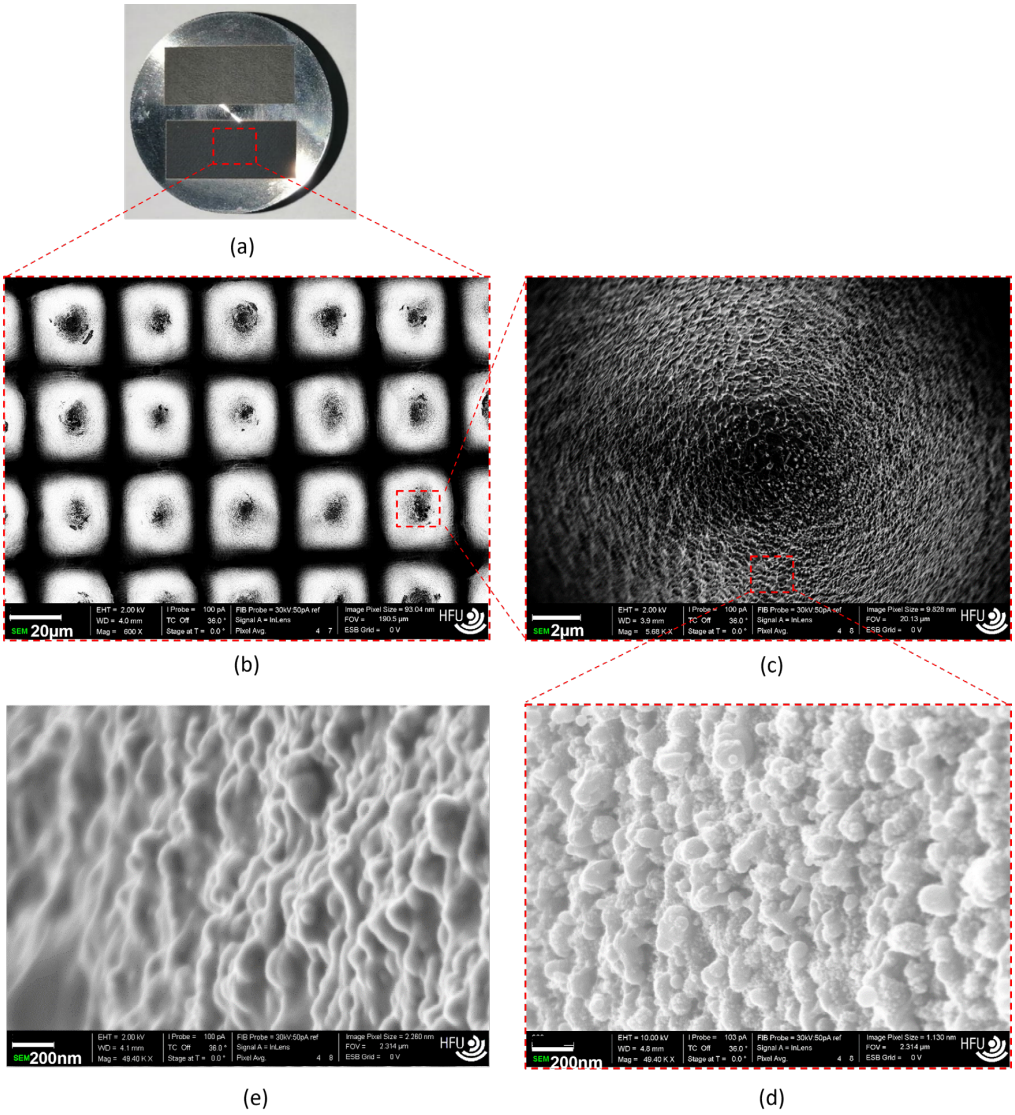

Figure 7. Investigation into nano-structures on the stamp—(**a**) laser-textured stamp, (**b**) pyramid texture array, (**c**) micro-feature, (**d**) ridge nano-structure before hot-embossing, and (**e**) ridge nano-structure after hot-embossing.

4. Conclusions

A novel, successful combined laser ablation and hot embossing process is presented in this study to produce hydrophobic surfaces on polymer workpieces. A femtosecond laser was utilized to texture the stamps with two different laser patterns. Four different types of polymers (ABS, PP, PA, and PC) were chosen as workpiece materials. The experimental results indicate that, among the five micro-features of the laser textures investigated herein, the height, landing length, and width are more decisive in achieving hydrophobicity. These features were completely transferred to the ABS and PP workpieces. The results showed that, for the PP samples compared to the ABS samples, the contact angles are considerably higher. Laser texturing for the ABS samples caused the contact angle to double.

Author Contributions: Conceptualization, B.A. and E.G.Z.; methodology, E.G.Z.; software, E.G.Z. and A.F.J.; validation, E.G.Z., A.F.J. and B.A.; formal analysis, E.G.Z.; investigation, E.G.Z. and A.F.J.; resources, B.A.; data curation, E.G.Z. and A.F.J.; writing—original draft preparation, E.G.Z.; writing—review and editing, E.G.Z. and B.A.; visualization E.G.Z. and B.A.; supervision B.A.; project administration, E.G.Z.; funding acquisition, B.A. All authors have read and agreed to the published version of the manuscript.

Funding: The results achieved in this study were part of the 'SuperSurf' project, funded by the Alfred Kärcher Foundation, for which the authors express their sincere gratitude.

Data Availability Statement: All the data are mentioned in the manuscript.

Acknowledgments: The results achieved in this study were part of the 'SuperSurf' project, funded by the Alfred Kärcher Foundation, for which the authors express their sincere gratitude. Also, many thanks to +GF+ Machining Solutions GmbH for their invaluable support in providing the laser machine. In addition, thanks are extended for the use of FIB-SEM, funded by the Deutsche Forschungsgemeinschaft (DFG, German Research Foundation), within the program Major Research Instrumentation (Project number: 505067193) under GG91b, and by the state of Baden-Württemberg, as well as by Furtwangen University. Thanks also to our colleague R. Bösinger for his help in preparing the SEM images. Many thanks also to Seyedehmina Mojabi for her help in experimentation.

Conflicts of Interest: The authors declare no conflict of interest.

References

1. Carré, A. (Ed.) *Superhydrophobic Surfaces*; VSP: Leiden, The Netherlands, 2009.
2. Chieng, B.W.; Ibrahim, N.A.; Ahmad Daud, N.; Talib, Z.A. Functionalization of Graphene Oxide via Gamma-Ray Irradiation for Hydrophobic Materials. In *Synthesis, Technology and Applications of Carbon Nanomaterials*; Elsevier: Amsterdam, The Netherlands, 2019; pp. 177–203.
3. Khan, S.A.; Boltaev, G.S.; Iqbal, M.; Kim, V.; Ganeev, R.A.; Alnaser, A.S. Ultrafast fiber laser-induced fabrication of superhydrophobic and self-cleaning metal surfaces. *Appl. Surf. Sci.* **2021**, *542*, 148560. [CrossRef]
4. Su, F.; Yao, K. Facile fabrication of superhydrophobic surface with excellent mechanical abrasion and corrosion resistance on copper substrate by a novel method. *ACS Appl. Mater. Interfaces* **2014**, *6*, 8762–8770. [CrossRef] [PubMed]
5. Limongi, T.; Schipani, R.; Di Vito, A.; Giugni, A.; Francardi, M.; Torre, B.; Allione, M.; Miele, E.; Malara, N.; Alrasheed, S.; et al. Photolithography and micromolding techniques for the realization of 3D polycaprolactone scaffolds for tissue engineering applications. *Microelectron. Eng.* **2015**, *141*, 135–139. [CrossRef]
6. Rodriguez, A.; Echeverría, M.; Ellman, M.; Perez, N.; Verevkin, Y.K.; Peng, C.S.; Berthou, T.; Wang, Z.; Ayerdi, I.; Savall, J.; et al. Laser interference lithography for nanoscale structuring of materials: From laboratory to industry. *Microelectron. Eng.* **2009**, *86*, 937–940. [CrossRef]
7. Liu, Y.; Yin, X.; Zhang, J.; Wang, Y.; Han, Z.; Ren, L. Biomimetic hydrophobic surface fabricated by chemical etching method from hierarchically structured magnesium alloy substrate. *Appl. Surf. Sci.* **2013**, *280*, 845–849. [CrossRef]
8. Zhao, Y.; Li, M.; Lu, Q.; Shi, Z. Superhydrophobic polyimide films with a hierarchical topography: Combined replica molding and layer-by-layer assembly. *Langmuir ACS J. Surf. Colloids* **2008**, *24*, 12651–12657. [CrossRef] [PubMed]
9. Sugioka, K.; Cheng, Y. Ultrafast lasers—Reliable tools for advanced materials processing. *Light Sci. Appl.* **2014**, *3*, e149. [CrossRef]
10. Malinauskas, M.; Žukauskas, A.; Hasegawa, S.; Hayasaki, Y.; Mizeikis, V.; Buividas, R.; Juodkazis, S. Ultrafast laser processing of materials: From science to industry. *Light Sci. Appl.* **2016**, *5*, e16133. [CrossRef] [PubMed]
11. Lei, S.; Zhao, X.; Yu, X.; Hu, A.; Vukelic, S.; Jun, M.B.G.; Joe, H.-E.; Yao, Y.L.; Shin, Y.C. Ultrafast Laser Applications in Manufacturing Processes: A State-of-the-Art Review. *J. Manuf. Sci. Eng.* **2020**, *142*, 031005. [CrossRef]
12. Alsaigh, R.A. Enhancement of Surface Properties Using Ultrashort-Pulsed-Laser Texturing: A Review. *Crystals* **2024**, *14*, 353. [CrossRef]

13. Moldovan, E.R.; Concheso Doria, C.; Ocaña, J.L.; Baltes, L.S.; Stanciu, E.M.; Croitoru, C.; Pascu, A.; Roata, I.C.; Tierean, M.H. Wettability and Surface Roughness Analysis of Laser Surface Texturing of AISI 430 Stainless Steel. *Material* **2022**, *15*, 2955. [CrossRef] [PubMed]
14. Gemini, L.; Faucon, M.; Romoli, L.; Kling, R. High throughput laser texturing of super-hydrophobic surfaces on steel. In Proceedings of the Laser-Based Micro- and Nanoprocessing XI, SPIE LASE, San Francisco, CA, USA, 28 January 2017; Klotzbach, U., Washio, K., Kling, R., Eds.; SPIE: Bellingham, WA, USA, 2017. 100921G. [CrossRef]
15. Gregorčič, P.; Conradi, M.; Hribar, L.; Hočevar, M. Long-Term Influence of Laser-Processing Parameters on (Super)hydrophobicity Development and Stability of Stainless-Steel Surfaces. *Materials* **2018**, *11*, 2240. [CrossRef] [PubMed]
16. Obilor, A.F.; Pacella, M.; Wilson, A.; Silberschmidt, V.V. Micro-texturing of polymer surfaces using lasers: A review. *Int. J. Adv. Manuf. Technol.* **2022**, *120*, 103–135. [CrossRef]
17. Riveiro, A.; Maçon, A.L.B.; Del Val, J.; Comesaña, R.; Pou, J. Laser Surface Texturing of Polymers for Biomedical Applications. *Front. Phys.* **2018**, *6*, 16. [CrossRef]
18. Worgull, M. *Hot Embossing. Theory and Technology of Microreplication*, 1st ed.; Micro & Nano Technologies; William Andrew: Oxford, UK, 2009.
19. Gong, Y.; Li, B.; Chen, L.; Lv, Q.; Wang, Q.; Liu, W.; Zou, L. Study on superhydrophobicity of hot embossed polytetrafluoroethylene/graphite composites. *J. Polym. Res.* **2023**, *30*, 168. [CrossRef]
20. Sun, J.; Li, H.; Huang, Y.; Zheng, X.; Liu, Y.; Zhuang, J.; Wu, D. Simple and Affordable Way To Achieve Polymeric Superhydrophobic Surfaces with Biomimetic Hierarchical Roughness. *ACS Omega* **2019**, *4*, 2750–2757. [CrossRef] [PubMed]
21. Victor, J.J.; Facchini, D.; Erb, U. A low-cost method to produce superhydrophobic polymer surfaces. *J. Mater. Sci.* **2012**, *47*, 3690–3697. [CrossRef]
22. Lee, H.-J.; Park, K. Development of composite micro-patterns on polymer film using repetitive ultrasonic imprinting. *Int. J. Precis. Eng. Manuf. Green Technol.* **2014**, *1*, 341–345. [CrossRef]
23. Wypych, G. *Handbook of Polymers*; ChemTec Publishing: Toronto, ON, Canada, 2012.
24. ASM International. *Engineered Materials Handbook. Desk Edition*, 1st ed.; ASM International: Materials Park, OH, USA, 1995.
25. Srinivasan, A.; Bandyopadhyay, S. (Eds.) *Advances in Polymer Materials and Technology*; Taylor & Francis CRC Press: Boca Raton, FL, USA, 2017.